0026-895X/06/7004-1369–1379$20.00
MOLECULAR PHARMACOLOGY
Copyright © 2006 The American Society for Pharmacology and Experimental Therapeutics
Mol Pharmacol 70:1369–1379, 2006

Vol. 70, No. 4
27672/3140481
Printed in U.S.A.

Role of Endogenous XAP2 Protein on the Localization and Nucleocytoplasmic Shuttling of the Endogenous Mouse Ah^{b-1} Receptor in the Presence and Absence of Ligand

Richard S. Pollenz, Sarah E. Wilson, and Edward J. Dougherty

Department of Biology, University of South Florida, Tampa, Florida

Received June 6, 2006; accepted July 11, 2006

ABSTRACT

Studies using transient expression systems have implicated the hepatitis B virus X-associated protein (XAP2) in the control of aryl hydrocarbon receptor (AHR) stability and subcellular location. Studies were performed in Hepa-1 cells to evaluate these functions of XAP2 on the mouse Ah^{b-1} receptor under endogenous stoichiometry. The Ah^{b-1} receptor is cytoplasmic, and it becomes predominantly nuclear after 30 to 60 min of ligand exposure with minimal degradation. During this time, XAP2 coprecipitates with the AHR, suggesting that it does not affect the nuclear localization of the liganded receptor. Overexpression of XAP2 in Hepa-1 cells does not result in increased association with the endogenous Ah^{b-1} complex or influence the receptors cytoplasmic localization. Knockdown of endogenous XAP2 by small interfering RNA results in ≥90% reduction in the amount of XAP2 associated with the endogenous Ah^{b-1} receptor complex. Despite the reduction in XAP2, the unliganded Ah^{b-1} receptor complex remains cytoplasmic, although inhibition of nuclear export results in accumulation of the receptor in the nucleus. Truncation of the C-terminal 305 amino acids of the Ah^{b-1} receptor (AHR$_{500}$) results in proteins that exhibit a predominantly nuclear localization and remain associated with the same level of endogenous XAP2 as full-length AHRs. Together, these results support a model in which the majority of the unliganded Ah^{b-1} receptor complexes are associated with XAP2, and the association prevents dynamic nucleocytoplasmic shuttling in the unliganded state. After ligand binding, XAP2 remains associated with the Ah^{b-1} receptor complex, and it does not impair nuclear translocation but may function to limit receptor "transformation".

The hepatitis B virus X-associated protein XAP2 (also termed ARA9 and AIP) was identified as a component of the latent aryl hydrocarbon receptor (AHR) complex using yeast two-hybrid screens and direct immunoprecipitation (Carver and Bradfield, 1997; Ma and Whitlock, 1997; Meyer et al., 1998). XAP2 shares sequence identity with the FKBP52 class of immunophilins, and this class of proteins is involved in subcellular trafficking, stability, and transactivation potential of steroid hormone receptors (for reviews, see Petrulis and Perdew, 2002; Davies and Sanchez, 2005). It has recently been determined that individuals with pituitary adenoma predisposition carry germline mutations within the XAP2 gene (Vierimaa et al., 2006). The mechanism of how loss of function of XAP2 results in pituitary adenoma predisposition and the possible relationship to the AHR is currently unclear; however, these findings highlight the importance of XAP2 and its associated proteins in normal cellular physiology.

Because XAP2 shares sequence identity with FKBP52, several studies have evaluated the function XAP2 with regard to the subcellular trafficking, stability, and transactivation potential of the AHR. However, with few exceptions, the analysis of AHR and XAP2 interactions has been carried out in vitro or in transient expression systems using the Ah^{b-1} receptor that is expressed in the C57BL/6 mouse strain. The results of these studies suggest that overexpression of XAP2 increases the level of Ah^{b-1} receptor protein and enhances the level of AHR-mediated gene regulation (Ma and Whitlock, 1997; Carver et al., 1998; Meyer and Perdew, 1999;

This work was supported in part by National Institutes of Health Grant ES10991 (to R.S.P.). Portions of this work were presented at the Society of Toxicology Annual Meeting, 5–9 March 2006, San Diego, CA.

Article, publication date, and citation information can be found at http://molpharm.aspetjournals.org.

doi:10.1124/mol.106.027672.

ABBREVIATIONS: XAP2, hepatitis B virus X-associated protein; AHR, Ah receptor; TCDD, 2,3,7,8-tetrachlorodibenzo-*p*-dioxin; DMSO, dimethyl sulfoxide; LMB, leptomycin B; GAR-HRP, goat anti-rabbit horseradish peroxidase; GAM-HRP, goat anti-mouse horseradish peroxidase; GAR-RHO, goat anti-rabbit IgG conjugated to rhodamine; PBS, phosphate-buffered saline; RIPA, radioimmunoprecipitation assay; TTBS, Tris-buffered saline/Tween 20; siCON, control small interfering RNA; BLOTTO, bovine lacto transfer optimizer; PAGE, polyacrylamide gel electrophoresis; ECL, enhanced chemiluminescence; siRNA, small interfering RNA; FITC, fluorescein isothiocyanate; h, human; YFP, yellow fluorescent protein; GFP, green fluorescent protein; NLS, nuclear localization sequence; NES, nuclear export sequence.

Bell and Poland, 2000; LaPres et al., 2000; Meyer et al., 2000). In addition, it has been reported that XAP2 expression can affect the subcellular localization of the Ah^{b-1} receptor and prevent it from undergoing dynamic nucleocytoplamsic shuttling in COS and HeLa cell lines (Kazlauskas et al., 2000, 2002; Berg and Pongratz, 2002; Petrulis et al., 2003). Although these findings are consistent with the function of immunophilin-like proteins in other receptor-mediated pathways (Davies and Sanchez, 2005), there is increasing evidence that the contribution of XAP2 to AHR function may be specific to the Ah^{b-1} class of receptors, and this role needs to be evaluated in an endogenous context.

To evaluate the role of endogenous XAP2 with different species of AHRs, studies were recently completed in cell lines that expressed endogenous mouse Ah^{b-1}, Ah^{b-2}, and rat AHRs and that contained similar levels of endogenous XAP2 (Pollenz and Dougherty, 2005). It is noteworthy that the unliganded mouse Ah^{b-2} and rat AHR complexes were associated with greatly reduced levels of XAP2 compared with Ah^{b-1} receptors. In addition, mouse Ah^{b-2} and rat AHR complexes exhibited dynamic nucleocytoplasmic shuttling in the absence of exogenous ligands, and the mouse Ah^{b-2} and rat AHRs exhibited a greater magnitude of ligand-induced degradation than Ah^{b-1} receptors. When the mouse Ah^{b-2} receptor was stably expressed in the C57BL/6 background, it was associated with minimal levels of XAP2, showed dynamic nucleocytoplasmic shuttling, and exhibited increased levels of ligand-induced degradation. Similar results have been reported for the human AHR, where the expression of XAP2 has been shown to have little impact on the subcellular localization or expression level of the receptor (Ramadoss et al., 2004). Together, these results demonstrate that there are striking differences in how XAP2 affects AHR-mediated signal transduction across species lines, and they suggest that endogenous XAP2 may function to modulate subcellular location and stability of only the Ah^{b-1} receptor complex. Because the concentration and subcellular locations of signaling proteins are critical parameters in their functionality, there are several key issues that need to be resolved with regard to XAP2 function on AHR-mediated signaling. First, it has not yet been determined whether XAP2 remains associated with the endogenous Ah^{b-1} receptor after ligand binding and nuclear translocation. Second, it is unclear whether the localization of the Ah^{b-1} receptors within the cytoplasm is solely dependent on its association with XAP2. Finally, it is of interest to investigate whether the reduced level of nucleocytoplasmic shuttling of the Ah^{b-1} receptor is due to its association with XAP2. The analysis of these questions will be important in further understating the role of XAP2 in the response of the AHR to toxicologically relevant chemicals as well as refining the mechanisms involved in ligand-induced degradation and gene regulation.

Materials and Methods

Materials. TCDD (98% stated chemical purity) was obtained from Radian Corp. (Austin, TX) and was solubilized in dimethyl sulfoxide (DMSO). Geldanamycin and leptomycin B (LMB) were purchased from Sigma-Aldrich (St. Louis, MO). pC3-NLS-GFP-GST-RevNES was a generous gift from Dr. Roland Stauber (Georg-Speyer-Haus, Frankfurt am Main, Germany). pCI-hXAP2 and pEYFP-XAP2-FLAG were generously provided by Dr. Gary Perdew (The Penn State University, University Park, PA).

Antibodies. Specific polyclonal antibodies against either the AHR (A-1, A-1A) or ARNT protein (R-1) are identical to those described previously (Pollenz et al., 1994; Holmes and Pollenz, 1997). Antibodies to XAP2 (Novus, Littleton, CO), actin (Sigma-Aldrich), and rat P4501A1 (Chemicon International, Temecula, CA) were purchased from commercial sources. For Western blot analysis, goat anti-rabbit or anti-mouse antibodies conjugated to horseradish peroxidase (GAR-HRP and GAM-HRP, respectively) were used. For immunohistochemical studies, goat anti-rabbit IgG conjugated to rhodamine (GAR-RHO) was used. Both of these reagents were purchased from Jackson ImmunoResearch Laboratories (West Grove, PA).

Buffers. PBS was 0.8% NaCl, 0.02% KCl, 0.14% Na_2HPO_4, and 0.02% KH_2PO_4, pH 7.4. SDS sample buffer was 60 mM Tris, pH 6.8, 2% SDS, 15% glycerol, 2 mM EDTA, 5 mM EGTA 10 mM dithiothreitol, and 0.005% bromphenol blue. Lysis buffer was 60 mM Tris, pH 6.8, 2% SDS, 15% glycerol, 2 mM EDTA, 5 mM EGTA, 10 mM dithiothreitol, 0.5% Nonidet P-40, 20 mM sodium molybdate, and 0.005% bromphenol blue. RIPA was 50 mM Tris, 150 mM NaCl, 0.2% Nonidet P-40, 20 mM sodium molybdate, and 20 mM DL-histidine, pH 7.4. TTBS was 50 mM Tris, 0.2% Tween 20, and 150 mM NaCl, pH 7.5. TTBS+ is 50 mM Tris, 0.5% Tween 20, and 300 mM NaCl, pH 7.5. BLOTTO is 5% dry milk in TTBS.

Cells and Growth Conditions. Wild-type Hepa-1c1c7 (Hepa-1) and type I (LA-I) Hepa-1 variants were a generous gift from Dr. James Whitlock, Jr. (Department of Pharmacology, Stanford University, Stanford, CA). LA-I cells stably expressing truncated AHR were produced as detailed previously (Pollenz et al., 2005). Wild-type Hepa-1 cells were propagated in Dulbecco's modified Eagle's medium supplemented with 10% fetal bovine serum. Stable lines were propagated in Dulbecco's modified Eagle's medium supplemented with 10% fetal bovine serum and 400 μg/ml G418 (Geneticin). All cell lines were passaged at 1-week intervals and used in experiments during a 3-month period at approximately 70 to 90% confluence. For treatment regimens, stated concentrations of TCDD, geldanamycin, or LMB were administered directly into growth media for the indicated incubation times.

Preparation of Total Cell Lysates. After treatment, cell monolayers were washed twice with PBS and detached from plates by trypsinization (0.05% trypsin, 0.5 mM EDTA). Cell pellets were washed with PBS and sonicated directly in 75 to 150 μl of ice-cold lysis buffer for 12 s. Lysates were immediately heated for 3 min at 100°C and then sonicated an additional 5 s. Samples were stored at −20°C until analysis.

Preparation of Cytosol and Immunoprecipitation. Cells were harvested by trypsinization as described above and disrupted by vortexing in RIPA buffer supplemented with 10 mM phenylmethylsulfonyl fluoride and 10 μM aprotinin. Cytosol was generated by centrifugation at 30,000*g* used for immunoprecipitation studies without prior freezing. Protein concentrations were determined using the Coomassie Plus assay (Pierce Chemical, Rockford, IL) with bovine serum albumin as the standard. In general, immunoprecipitations were carried out with 600 μg of cytosol in a total of 600 μl of RIPA buffer supplemented with 20 μg/ml bovine serum albumin and 20 mM histidine. Triplicate samples were incubated with either affinity pure A1-A (AHR) IgG (5 μg) or affinity pure preimmune rabbit IgG (5 μg) for 90 min at 4°C. Then, 25 μl of protein A/G agarose (Pierce Chemical) was added, and the incubation was continued an additional 90 min at 4°C. Pellets were washed with TTBS containing 20 mM sodium molybdate three times for 5 min at 4°C, and protein was eluted by boiling in 30 μl of SDS sample buffer. Samples were then centrifuged at 30,000*g*, and the triplicate samples were combined. Next, 15 to 20 μl of sample was resolved by discontinuous polyacrylamide slab gels (SDS-PAGE) and blotted to nitrocellulose. Due to the large amount of total protein needed for each immunoprecipitation experiment, it was not possible to do duplicate samples. However, all immunoprecipitation studies were repeated at least two times.

Western Blot Analysis and Quantification of Protein. Equal amounts of protein were resolved by SDS-PAGE and electrophoretically transferred to nitrocellulose. Immunochemical staining was carried out with varying concentrations of primary antibody (see text and figure legends) in BLOTTO buffer supplemented with 20 mM DL-histidine for 1 to 2 h at 22°C. Blots were washed with three changes of TTBS+ for a total of 45 min. The blot was incubated in BLOTTO buffer containing a 1:10,000 dilution of appropriate peroxidase-conjugated secondary antibody for 1 h at 22°C and washed in three changes of TTBS+ described as described above. Before detection, the blots were rinsed in PBS. Bands were visualized with the enhanced chemiluminescence (ECL) kit as specified by the manufacturer (GE Healthcare, Little Chalfont, Buckinghamshire, UK). Multiple exposures of each set of samples were produced. The relative concentration of target protein was determined by computer analysis of the exposed film as detailed previously (Pollenz, 1996; Holmes and Pollenz, 1997; Pollenz et al., 1998).

Immunofluorescence Staining and Microscopy. All immunocytochemical procedures (cell plating, fixation, and staining) were carried out as described previously (Pollenz et al., 1994; Pollenz, 1996; Holmes and Pollenz, 1997). Cells were observed on an Olympus IX70 microscope (Olympus, Tokyo, Japan). On average, 5 to 10 fields (15–25 cells per field) were evaluated on each coverslip, and three to four fields were photographed with a digital camera at the same exposure time to generate the raw data. Nuclear fluorescence intensities of 50 to 75 cells in three to four distinct fields of view were obtained using MicroSuite image analysis software (Olympus America Inc., Melville, NY).

Transfection and RNA Interference. Annealed small interfering RNA (siRNA) complexes containing 21-base pair regions of identity to regions of the murine XAP2 or an annealed 21-base pair RNA to sequence not present in the mouse genome (siCON) were purchased from Ambion (Austin, TX). siRNA (final concentration, 50–100 nM) or plasmid DNA (1 μg/well) was transfected into 35-mm dishes containing 1 to 2 $\times$ 10^5 cells using Lipofectamine reagent (Invitrogen, Carlsbad, CA). To monitor transfection efficiency, the BLOCK-IT FITC-labeled RNA reagent (Invitrogen) was included in the transfection cocktail. Twenty-four to 48 h after transfection, cells were treated as detailed in the text, and total cell lysates were harvested for Western blotting, or the cells were fixed and stained as detailed above. The efficiency of siRNA gene knockdown of XAP2 was determined by Western blotting. Transfection efficiency was monitored by microscopy using FITC-labeled RNA (Clontech, Mountain View, CA). In general, transfection efficiency in all experiments was >85%.

Statistical Analysis. Target protein bands from total cell lysates were normalized to internal standards (actin) to generate normalized densitometry units. Target protein values or nuclear fluorescence intensities were compared by analysis of variance and Tukey-Kramer multiple comparison tests using InStat software (GraphPad Software Inc., San Diego, CA). Results are presented as mean ± S.E. A probability value of <0.05 was considered significant.

Results

XAP2 Remains Associated with the Ah^{b-1} AHR Complex after Ligand Binding and Nuclear Translocation. Studies using transient expression experiments suggest that XAP2 functions in AHR-mediated signal transduction by stabilizing the latent AHR complex and modulating subcellular localization (Ma and Whitlock, 1997; Carver et al., 1998; Meyer and Perdew, 1999; Bell and Poland, 2000; Kazlauskas et al., 2000, 2002; LaPres et al., 2000; Meyer et al., 2000; Berg and Pongratz, 2002; Petrulis et al., 2003). However, the function that XAP2 exerts on nuclear translocation of the endogenous Ah^{b-1} AHR after ligand binding remains to be resolved. To begin to address this question, it is first necessary to determine the precise time line of nuclear localization and degradation of the endogenous Ah^{b-1} AHR after ligand exposure. Hepa-1 cells were treated with TCDD for 0 to 300 min, and the endogenous Ah^{b-1} AHR was visualized by immunocytochemistry or quantified in total cell lysates using Western blotting. The time course of nuclear localization is presented in Fig. 1A. In untreated cells (time = 0), it can be observed that the endogenous Ah^{b-1} AHR is localized predominantly within the cytoplasmic compartment. After 30 to 45 min of ligand stimulation, the fluorescence intensity associated with the AHR becomes predominantly nuclear and then declines (Fig. 1A). These results are in agreement with previous analyses of the endogenous Ah^{b-1} AHR as well as studies that have assessed the localization of AHR-GFP chimeras (Pollenz et al., 1994; Pollenz, 1996; Davarinos and Pollenz, 1999; Elbi et al., 2002; Song and Pollenz, 2002; Pollenz and Dougherty, 2005).

To obtain a quantitative measure of the change in AHR localization, image analysis was used to measure the relative fluorescence intensities of the Hepa-1 nuclei. The average values for 75 to 100 individual cells were then plotted as a function of time, and a representative experiment is shown in Fig. 1B. The results indicate that the fluorescence intensity of the nucleus peaks 45 to 60 min after ligand stimulation and then declines over the remaining time frame to levels at or below those of the time = 0 cells. Because there is no recovery of the fluorescence to other cellular compartments throughout the time course, these results are consistent with a nuclear translocation event that is followed by degradation. To validate this hypothesis, quantitative Western blotting was carried out on total cell lysates that were prepared from Hepa-1 cells exposed to TCDD over the identical time frame shown in Fig. 1A. A representative Western blot is shown in Fig. 1C, and the quantified results are presented in Fig. 1B. As expected, the overall level of AHR protein is reduced by approximately 82% after 240 to 300 min of TCDD exposure, but the key finding of these studies is that the degradation of the AHR does not occur immediately after ligand exposure. Indeed, the level of AHR declines by only 20% during the first 75 min of ligand exposure with the majority of the AHR protein degraded between the 75- and 240-min time points. It is noteworthy that the time course of AHR degradation paralleled the reduction that was observed in the nuclear fluorescence. These results establish that during the first 60 to 75 min of ligand exposure, the Ah^{b-1} receptor protein is translocated to the nuclear compartment without undergoing high levels of degradation. Therefore, the first 60 to 75 min of ligand exposure provide a window of time for the analysis of changes within the endogenous Ah^{b-1} receptor complex that will not be confounded by large reductions in the basal level of the protein.

The next series of studies was designed to assess the association of XAP and ARNT with the soluble AHR complex during the first 75 min of ligand exposure. Hepa-1 cells were stimulated with TCDD for 0 to 75 min, harvested, and then lysed by vortexing in buffer containing nonionic detergent. The supernatant fractions were incubated with antibodies specific to the AHR, and these complexes were precipitated with protein A/G agarose as described under *Materials and Methods*. Identical samples were then evaluated for level of XAP2, AHR, and ARNT by Western blotting. Cell disruption by this method has been found to be sufficient to allow

redistribution of soluble proteins from the nucleus (Paine et al., 1983; Pollenz et al., 1994; Holmes and Pollenz, 1997); thus, any AHR that was translocated to the nucleus but was not tightly associated with nuclear structures should partition to the supernatant fraction and be available for immunoprecipitation. This study was carried out three times and a representative experiment is shown in Fig. 2, A and B.

The results show that AHR, XAP2, and ARNT are present in all of the supernatant fractions and that the AHR can be specifically precipitated from each. It is noteworthy that XAP2 is coprecipitated from all of the fractions, whereas ARNT coprecipitates from the fractions prepared from cells that were exposed to ligand for 20, 40, 60, and 75 min. Because the results in Fig. 1 clearly show that the AHR is predominantly nuclear after 45 min of ligand exposure, these findings suggest that there are multiple pools of soluble AHR complexes in the nucleus of the Hepa-1 cell after ligand exposure and that some of the complexes remain associated with XAP2. To determine whether there were differences in the relative ratio of XAP2/AHR at each time point, the blots presented in Fig. 2A were quantified by densitometry, and the results are presented in Fig. 2B. The results show that over the time course of study, the level of AHR is reduced by approximately 20%, whereas the level of XAP2 that is coprecipitated is reduced by approximately 40% between the 40- to 75-min time points. Thus, a portion of the XAP2 is being lost from the AHR complex over time. However, the level of ARNT that is coprecipitated increases over the time course. This type of trend suggests a model in which the soluble AHR complex not associated with XAP2 is associated with ARNT. It is important to note, however, that even though the level of XAP2 associated with the AHR core complex is declining during the time course, XAP2 remains associated with a significant proportion of the AHR complex even after 75 min of ligand exposure.

Figure 1C shows that the endogenous Ah^{b-1} receptor is not fully degraded after ligand exposure and that a small fraction of receptors (15–20%) remains in the cells 6 h later. Similar results have been reported in cells treated with ligands for 24 to 48 h and beyond (Giannone et al., 1995; Pollenz, 1996;

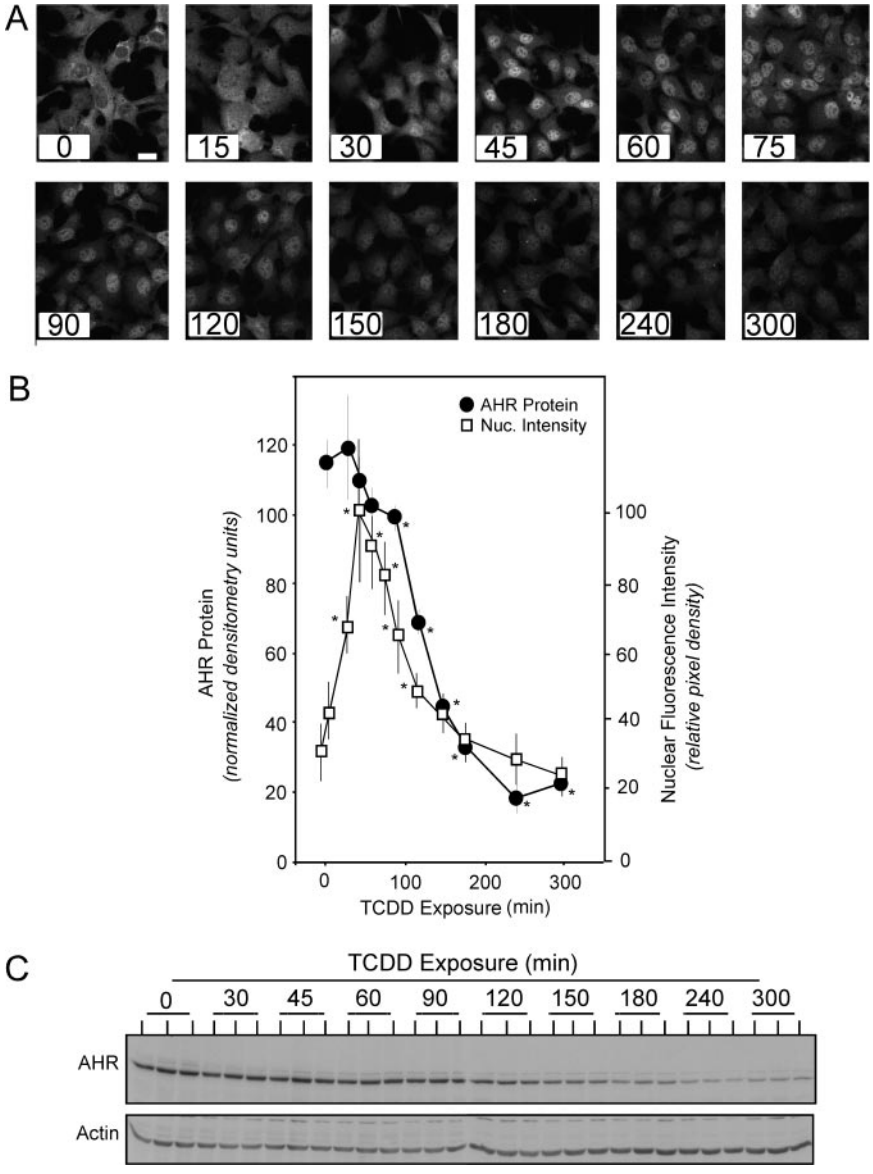

Fig. 1. Analysis of AHR localization and degradation in Hepa-1 cells. A, Hepa-1 cells were grown on glass coverslips and exposed to 0.1% DMSO for 300 min (time = 0) or 2 nM TCDD for the indicated times. Cells were fixed and then incubated with 1.0 μg/ml A-1 IgG and visualized with GAR-RHO IgG (1:400). All panels were photographed under identical exposures. Scale bar, 10 μm. Numbers represent TCDD exposure times in minutes. B, nuclear fluorescence intensities were determined for the cells presented in A. Fifty to 75 cells in three to four distinct fields of view were quantified using MicroSuite image analysis software, and the average ± S.E. is plotted as relative pixel density versus time. The level of AHR and actin protein shown in C was determined by computer densitometry as detailed under *Materials and Methods*. Normalized values are plotted as the average ± S.E. three individual samples. Statistically different from time 0 samples, *, $p > 0.005$. C, triplicate plates of Hepa-1 cells were exposed to 0.1% DMSO for 300 min (time = 0) or 2 nM TCDD for the indicated times. Equal amounts of total cell lysates were then resolved by SDS-PAGE, blotted, and stained with 1.0 μg/ml A-1A IgG and β-actin IgG (1:1000). Reactivity was visualized by ECL with GAR-HRP IgG (1:10,000), and bands were quantified and normalized as detailed in text.

Pollenz et al., 1998). These findings are in contrast to those in cell lines expressing endogenous Ah^{b-2} or rat AHRs where the AHR is degraded by 95 to 100% after only 2 to 4 h of ligand exposure (Pollenz, 1996; Davarinos and Pollenz, 1999; Pollenz and Dougherty, 2005). Thus, it was pertinent to determine whether XAP2 was associated with the population of Ah^{b-1} receptors that remained in Hepa-1 cells after prolonged ligand exposure. Hepa-1 cells were treated with TCDD for 4 h, and supernatant fractions were prepared. The results show that the level of endogenous AHR in the input fraction prepared from the TCDD-treated cells is reduced by approximately 85% (Fig. 2C). The samples were then immunoprecipitated with the after modification: 7-fold more sample protein was used to precipitate the AHR from the TCDD-treated samples compared with the controls, whereas the overall volume and amount of AHR IgG used in the experiment were held constant. This modification allowed the overall level of AHR being precipitated to be equal between the two samples. The results show that under these experimental conditions, nearly equal levels of AHR were precipitated from each fraction, and a comparatively equal amount of XAP2 was also coprecipitated from each sample (Fig. 2C). Thus, the relative ratio of XAP2/AHR was the same in both the control and TCDD-treated samples (Fig. 2D). Therefore, these findings suggest that there is a small population of Ah^{b-1} receptors that are recalcitrant to the ligand-induced degradation events and that they remain associated with XAP2.

Exogenous Expression of XAP2 Does Not Affect the Localization of the Endogenous Ah^{b-1} AHR Complex or the Level of XAP2 Associated with the Ah^{b-1} AHR Complex. Previous results suggest that the entire pool of Ah^{b-1} receptor complexes in Hepa-1 cells is not associated with XAP2 and that there are populations of receptors that reside in the nucleus (Petrulis et al., 2000). Thus, based on these results, it would be predicted that expression of exogenous XAP2 in the Hepa-1 line would result in increased association of XAP2 with the endogenous Ah^{b-1} receptor complex, increased distribution of the complex to the cytoplasm, and possibly increased levels of AHR protein. Thus, Hepa-1 cells were transfected with vectors that express either human XAP2 (hXAP) or yellow fluorescent protein-tagged hXAP (YFP-XAP2). After 24 h, total cells lysates were prepared and evaluated by Western blotting, or cells were fixed and stained

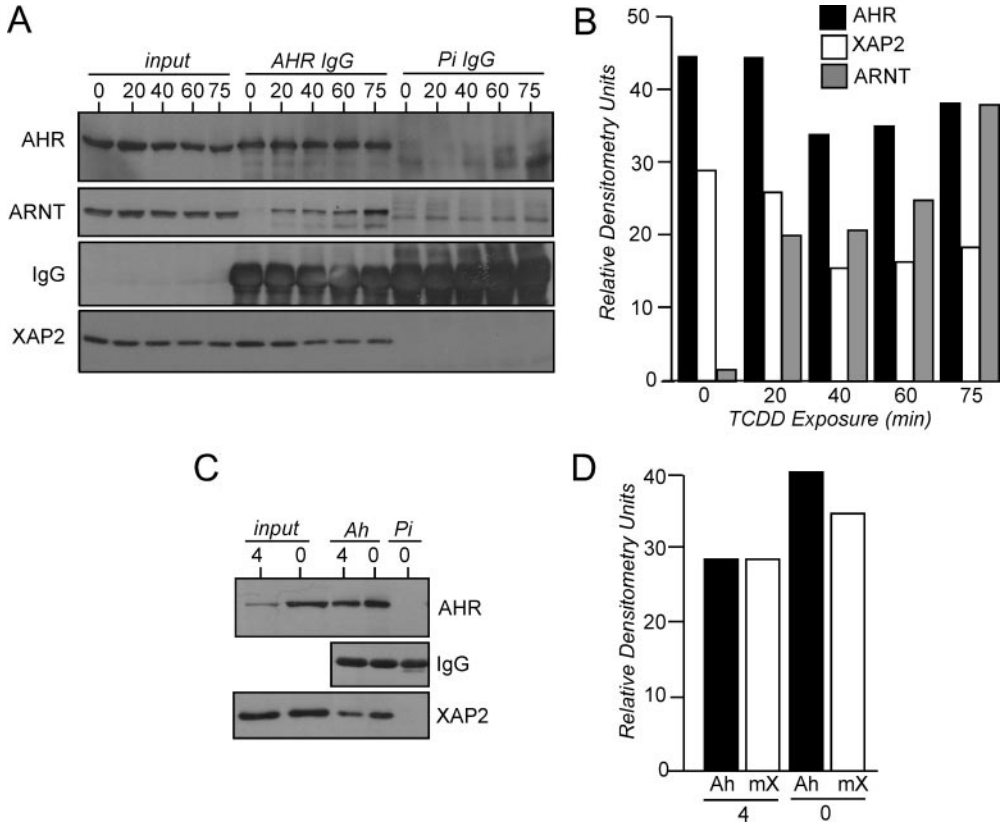

Fig. 2. Association of endogenous AHR, ARNT, and XAP2 in Hepa-1 cells treated with TCDD. A, cytosol was prepared from Hepa-1 cells treated with either 0.1% DMSO for 75 min or 2 nM TCDD for 20, 40, 60, or 75 min. Then, 600 μg of cytosol from each time point was precipitated with either AHR (AHR-IgG) or preimmune IgG (Pi-IgG) as detailed under *Materials and Methods*. Each of the precipitated samples as well as 15 μg of cytosol (input) was resolved by SDS-PAGE and blotted. Blots were stained with either 1.0 μg/ml A-1A IgG, 1.0 μg/ml R-1 IgG, or XAP2 mouse IgG$_1$ (1:750), and reactivity was visualized by ECL with GAR-HRP or GAM-HRP IgG (1:10,000). The IgG bands are presented to show the consistency of the precipitations. B, computer densitometry was used to determine the relative level of AHR, ARNT, or XAP2 protein present in the precipitated samples presented on the blot in A. Each column represents the relative densitometry units of an individual band and can be used to evaluate differences in the ratio of XAP2/AHR or ARNT/AHR in the different samples. However, because of the difference in the sensitivity of each antibody for its target protein, the ratio does not represent the absolute number of protein molecules. C, cytosol was prepared from Hepa-1 cells treated with either 0.1% DMSO or 2 nM TCDD for 4 h. Then, 600 μg of control (0) and 4.2 mg of 4-h cytosol (4) were precipitated as described in A. The precipitated samples as well as 15 μg of cytosol (input) were resolved by SDS-PAGE, blotted, and the identical samples were stained for either AHR or XAP as detailed above. Ah, precipitated with A-1A (AHR) IgG; Pi, precipitated with preimmune rabbit IgG. D, computer densitometry was used to determine the relative level of AHR and XAP2 protein present in the precipitated samples as described in B. Ah, relative level of AHR protein; mX, relative level of XAP2 protein. Note that the relative ratio of XAP2/AHR is unchanged in the 4-h samples compared with the controls.

to assess the localization of the endogenous AHR. The hXAP constructs used for these studies have been shown to interact with the mouse AHR and to influence its subcellular localization and expression level in transient transfection assays (Meyer et al., 2000; Petrulis et al., 2000; Ramadoss et al., 2004). Figure 3A shows that the overall level of total XAP protein can be elevated 3- to 4-fold when Hepa-1 cells are transfected with vectors that express hXAP or YFP-XAP2 and that the increased level XAP2 protein does not result in an elevation in the concentration of the endogenous Ah^{b-1} receptor. To determine whether the increased level of XAP2 expression influenced the subcellular localization of the unliganded Ah^{b-1} receptor, transfected cells were stained for the AHR. Representative images are shown in Fig. 3B. As shown in Fig. 1, the endogenous Ah^{b-1} receptor exhibited a predominantly cytoplasmic staining pattern, and populations expressing increased levels of XAP2 showed no significant changes in this pattern. It is noteworthy that the inability to observe changes in the subcellular localization of the endogenous Ah^{b-1} complex was not due to low levels of transfection efficiency, because >85% of the population showed an FITC signal from the tagged RNA that was included in the transfection cocktail. In addition, the cytoplasmic localization of the Ah^{b-1} receptor is unaltered in cells that express YFP-XAP2 compared with cells that were not transfected (Fig. 3B). Thus, these results show that increased expression of hXAP2 in Hepa-1 cells does not affect the concentration or localization of the endogenous Ah^{b-1} receptor.

Because the increased expression of hXAP did not seem to influence the subcellular location of the endogenous Ah^{b-1} receptor, it was pertinent to determine whether increased expression of hXAP resulted in an increase in the level of total XAP2 associated with the Ah^{b-1} complex. Therefore, transfected cells were lysed, the AHR complex was immunoprecipitated with AHR antibodies, and the samples were evaluated for AHR and XAP2 protein by Western blotting. This study was carried out two times. A representative experiment is presented in Fig. 4A, and the quantified results are presented in Fig. 4B. In the study presented, the level of hXAP overexpression was approximately 3.5-fold above the level of endogenous mXAP2, and the hXAP can be distinguished from the endogenous mXAP2, because it resolves at a slightly lower molecular mass. It is interesting that when hXAP was expressed in the Hepa-1 cells, both hXAP and mXAP2 were coprecipitated with the AHR. However, despite the increased level of total XAP2 protein that was present in the transfected population, the level of associated hXAP did not increase the total amount of XAP2 associated with the AHR complex, but it replaced a similar amount of endogenous mAXP2 (Fig. 4, A and B). Thus, the total amount of XAP2 associated with the endogenous AHR complex was not elevated above the level found in control cells (note that the relative ratio of total XAP2/AHR in the four samples is essentially the same). Together, these results support the hypothesis that the entire population of endogenous Ah^{b-1} complex in Hepa-1 cells is associated with XAP2.

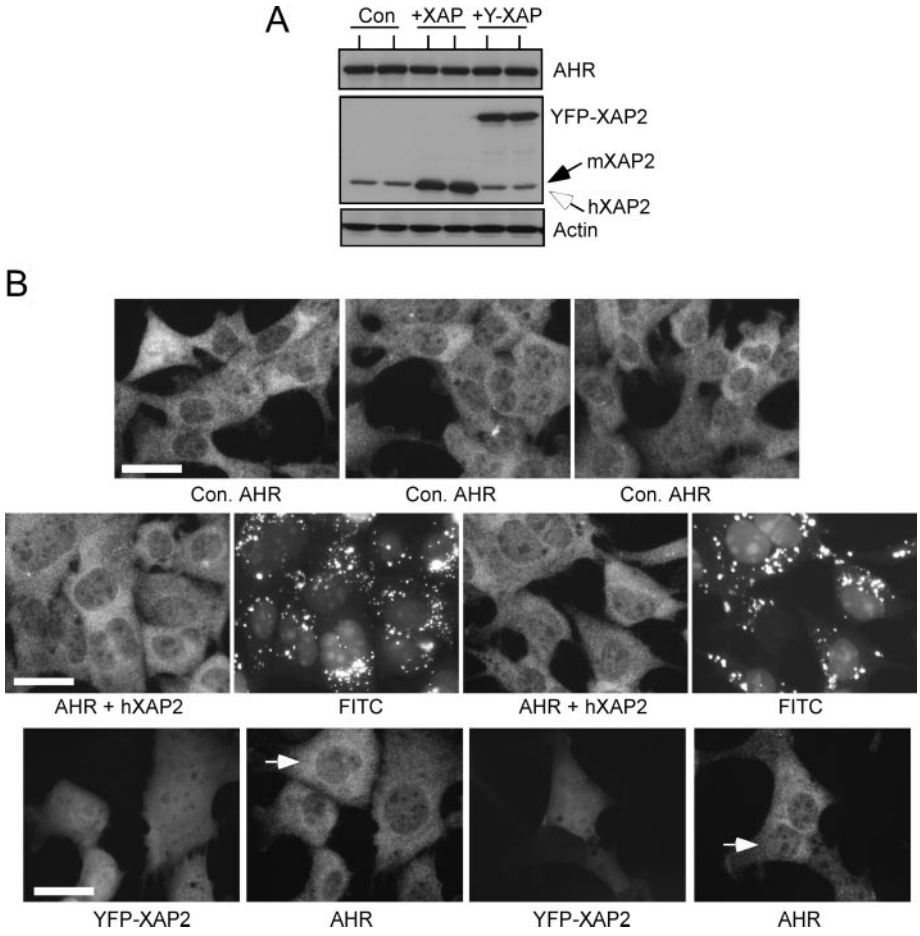

Fig. 3. Localization of endogenous Ah^{b-1} receptor in Hepa-1 cells expressing hXAP. Hepa-1 cells were transfected with pCI-hXAP2 along with FITC-labeled RNA (BLOCK-IT), pEYFP-XAP2-FLAG, or control vector pCDNA3.1 as detailed under *Materials and Methods.* After 24 h, populations of cells were either harvested for the generation of total cell lysates or fixed for immunocytochemical staining. A, equal amounts of the indicated samples were resolved by SDS-PAGE and blotted. Blots were stained with either 1.0 μg/ml A-1A IgG, XAP2 mouse IgG_1 (1:750), or anti-actin IgG (1:1000), and reactivity was visualized by ECL with GAR-HRP or GAM-HRP IgG (1:10,000). Con, cells transfected with pcDNA3.1; +XAP, cells transfected with pCI-hXAP2 and BLOCK-IT; +Y-XAP, cells transfected with pEYFP-hXAP2-FLAG. B, exact Hepa-1 populations that were transfected as detailed in A were fixed and stained for the AHR with 1.0 μg/ml A-1 IgG and visualized with GAR-RHO IgG (1:400). Con AHR, AHR staining pattern in cells transfected with pcDNA3.1; AHR + hXAP2, AHR staining pattern in cells transfected with pCI-hXAP2 and BLOCK-IT; FITC, FITC labeling of the exact field presented to the left to illustrate the transfection efficiency of the experiment; YFP-XAP2, pattern of the expressed EYFP-XAP2-FLAG; AHR, AHR staining pattern of the exact field presented to the left. The arrows indicate cells that are not expressing the EYFP-XAP2-FLAG protein. Scale bar, 10 μm.

Reduction of Endogenous XAP2 with siRNA Does Not Affect the Localization of the Endogenous Ah^{b-1} Complex but Stimulates Its Nucleocytoplasmic Shuttling. The previous results suggest that the entire population of Ah^{b-1} complex is associated with XAP2 and that under endogenous stoichiometry the XAP2 protein remains associated with the Ah^{b-1} receptor after the ligand-induced nuclear translocation event. Thus, it was pertinent to assess whether the cytoplasmic localization of the unliganded Ah^{b-1} complex and its inability to undergo dynamic nucleocytoplasmic shuttling was due to its association with XAP2. The strategy for these studies was to reduce the level of endogenous XAP2 protein by transfection of siRNAs specific to XAP2 and then to assess the localization of the AHR by immunocytochemistry. However, it was first necessary to demonstrate that the siRNA protocol would lead to a reduction in the level of XAP2 actually *associated* with the endogenous AHR complex and also to establish conditions to inhibit nucleocytoplasmic shuttling in the Hepa-1 cell line.

To establish that endogenous AHR complexes could be generated that were associated with reduced level of XAP2, Hepa-1 cells were transfected with control (siCON) or XAP2-specific (siXAP2) siRNA as detailed under *Materials and Methods* and allowed to recover for 48 h. Supernatant fractions were prepared from the transfected cells, and immunoprecipitation studies carried out as described previously. A representative experiment is shown in Fig. 4A. The input samples demonstrate that Hepa-1 cells transfected with siXAP2 exhibit >80% reduction in the level of endogenous XAP2 compared with cells transfected with siCON. When the AHR was immunoprecipitated from these samples, the amount of XAP2 associated with the endogenous AHR complex was reduced by >90% in comparison with controls (Fig. 5, A and B). Thus, these studies confirm that reductions in the basal levels of XAP2 are reflected in equal or greater reductions in the level of XAP2 associated with the unliganded AHR core complex.

It was next important to determine conditions to inhibit nucleocytoplasmic shuttling behavior in the Hepa-1 cell line. For these studies, Hepa-1 cells were transfected with the pC3-NLS-GFP-GST-RevNES expression construct that expresses a chimeric GFP-GST fusion protein containing both nuclear localization (NLS) and nuclear export (NES) sequences (Knauer et al., 2005). Cells were then treated with vehicle control or 1 nM leptomycin B for 2 h to inhibit chromosomal region maintenance-1-mediated nuclear export (Kudo et al., 1997, 1998). The location of the GFP was monitored by fluorescence microscopy, and representative photographs are shown in Fig. 5C. It is noteworthy that the GFP chimera exhibited a predominantly cytoplasmic localization in the untreated Hepa-1 line, despite the presence of both NLS and NES domains (Fig. 5C, control). In contrast, when Hepa-1 cells were treated with LMB, the GFP chimera became rapidly localized within the nuclear compartment (Fig. 5C, LMB). Thus, these experiments establish that proteins can undergo rapid nucleocytoplasmic shuttling behavior in the Hepa-1 line and that the process can be efficiently inhibited by using 1 nM LMB.

Having established conditions to reduce the level of XAP2 associated with the core AHR complex and also inhibit nuclear export, studies were designed to assess whether a reduction in XAP2 would affect the shuttling behavior of the endogenous AHR. Hepa-1 cells were transfected with siCON or siXAP2 as well as marker RNA tagged with FITC to monitor transfection efficiency. Forty-eight hours later, cells were treated with 1 nM LMB or vehicle control for 4 h and then fixed and stained for AHR. In addition, several duplicate plates of cells were used to generate total cell lysates so that the level of AHR and XAP2 protein could be evaluated by Western blotting. A representative experiment is shown in Fig. 6. The Western blot results confirm that the level of endogenous XAP2 was reduced by >80% in cells transfected with siXAP2 (Fig. 6A). It is noteworthy that reductions in XAP2 do not seem to affect the distribution of the unliganded AHR complex (Fig. 6B). Indeed, cells with reduced XAP2 show the same cytoplasmic distribution of the AHR as cells

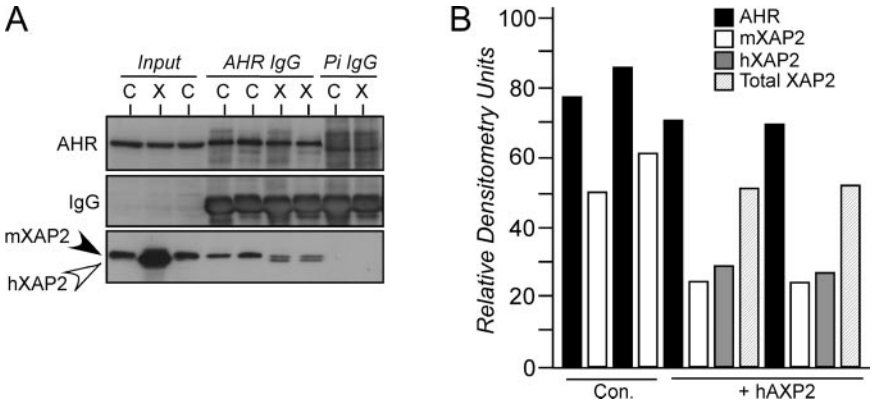

Fig. 4. Association of endogenous XAP2 with AHR in Hepa-1 cells transfected with hXAP expression vectors. Hepa-1 cells were transfected with pCI-hXAP2 or control vector pcDNA3.1 as detailed under *Materials and Methods.* After 24 h, populations of cells were harvested, and cytosol was generated for immunoprecipitation experiments. A, 600 μg of cytosol from the indicated samples was precipitated in duplicate with either AHR (AHR-IgG) or preimmune IgG (Pi-IgG) as detailed under *Materials and Methods*. Each of the precipitated samples as well as 15 μg of cytosol (input) was resolved by SDS-PAGE and blotted. Blots were stained with either 1.0 μg/ml A-1A IgG or XAP2 mouse IgG$_1$ (1:750), and reactivity was visualized by ECL with GAR-HRP or GAM-HRP IgG (1:10,000). mXAP2, endogenous mouse XAP2; hXAP2, exogenous human XAP2; and AHR (AHR). The IgG bands are presented to show the consistency of the precipitations. C, samples from cells transfected with pcDNA3.1; X, samples from cells transfected with pCI-hXAP2. B, computer densitometry was used to determine the relative level of AHR or XAP2 protein present in the precipitated samples presented on the blot in A. Each column represents the relative densitometry units of an individual band and can be used to evaluate differences in the ratio of XAP2/AHR in the different samples. However, because of the difference in the sensitivity of each antibody for its target protein, the ratio does not represent the absolute number of protein molecules. Note that the XAP2/AHR ratio is essentially unchanged in all the samples.

transfected with control siRNA. In contrast, there is a marked increase in the nuclear localization of the AHR when cells transfected with siXAP2 are treated with LMB for 4 h. The change in localization of the AHR is not observed in LMB-treated cells transfected with siCON. It is important to note that the transfection efficiency in the experiment presented in Fig. 6 was approximately 90% and is illustrated by the high number of cells that are labeled with the FITC-tagged RNA used to monitor transfection. Together, these results suggest that when endogenous XAP2 is reduced in the Hepa-1 cell line, the endogenous Ah^{b-1} receptor undergoes a moderate level of nucleocytoplasmic shuttling, yet retains a predominantly cytoplasmic localization.

Truncation of the C-Terminal Portion of the Ah^{b-1} AHR Results in Constitutively Nuclear AHR That Is Associated with XAP2. To gain additional insight into the role that the endogenous XAP2 plays in the subcellular location of the AHR, stable cell lines were generated that expressed Ah^{b-1} receptors that carried C-terminal truncations (Fig. 7A). These cell lines have been described previously (Pollenz et al., 2005) and are useful for the analysis of XAP2 function on nuclear translocation, because the truncated AHRs show distinct subcellular localization. Figure 7B shows the localization of AHR_{WT}, AHR_{500}, and AHR_{640} in cells that have been fixed and stained with AHR antibodies. It can be observed that AHR_{500} is localized predominantly within the nucleus in the absence of exogenous ligand, whereas AHR_{WT} and AHR_{640} show the expected cytoplasmic localization. To confirm that the nuclear localization of AHR_{500} was not an artifact of integration events during construction of the cell line, six independent lines were evaluated, and all exhibited the nuclear distribution shown in Fig. 7B. Thus, it was pertinent to determine whether the unliganded AHR_{500} was associated with the same level of XAP2 as AHR_{640} or AHR_{WT}. Supernatant fractions were prepared from the different cell lines, and immunoprecipitation studies were carried out as described previously. Figure 7C shows that the level of AHR and XAP2 expression in each of the lines is consistent and

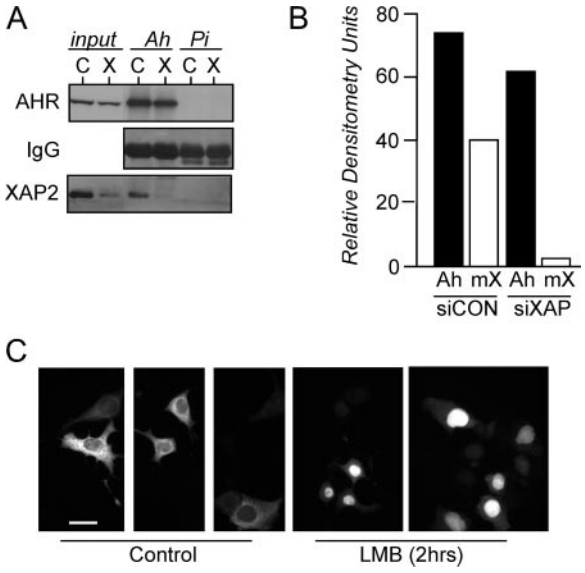

Fig. 5. Reduction of endogenous XAP2 by siRNA knockdown and analysis of nucleocytoplasmic shuttling in Hepa-1 cells. A, Hepa-1 cells were transfected with siRNA specific to XAP2 or control siRNA as detailed under *Materials and Methods*. Forty-eight hours later, cytosol was prepared, and 600 μg was precipitated with either AHR (Ah-IgG) or preimmune IgG (Pi-IgG) as detailed under *Materials and Methods*. Each of the precipitated samples as well as 15 μg of cytosol (input) was resolved by SDS-PAGE and blotted. Blots were stained with either 1.0 μg/ml A-1A IgG or XAP2 mouse IgG_1 (1:750), and reactivity was visualized by ECL with GAR-HRP or GAM-HRP IgG (1:10,000). The IgG bands are presented to show the consistency of the precipitations. C, cells transfected with control siRNA; X, cells transfected with XAP2 siRNA. B, computer densitometry was used to determine the relative level of AHR or XAP2 protein present in the precipitated samples presented on the blot in A. Each column represents the relative densitometry units of an individual band and shows that the ratio of XAP2/AHR has changed in the siXAP samples. Ah, level of AHR protein; mX, level of XAP2 protein. C, Hepa-1 cells were transfected with pC3-NLS-GFP-GST-RevNES and allowed to recover for 24 h. Cells were treated with either 0.1% methanol or 1 nM LMB for 2 h, and the live cells were visualized by fluorescence microscopy. Scale bar, 10 μm.

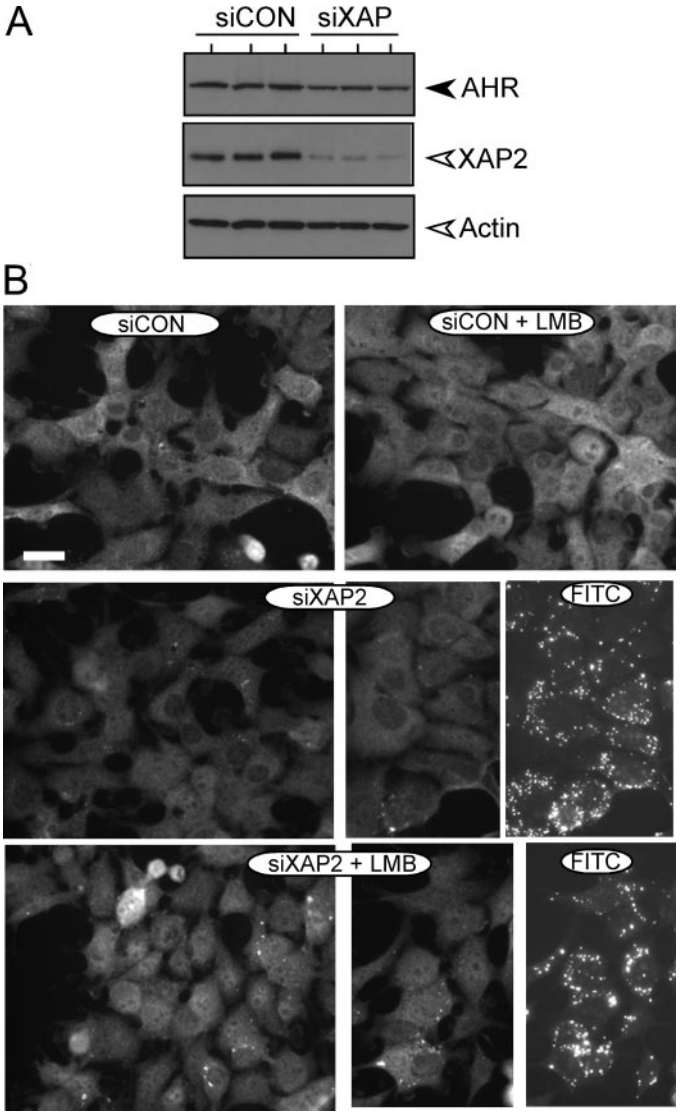

Fig. 6. Subcellular localization of AHR in cells with reduced levels of XAP2. Hepa-1 cells were transfected with siRNA specific to XAP2 or control siRNA along with FITC-labeled RNA (BLOCK-IT) as detailed under *Materials and Methods*. Forty-eight hours later, cells were treated with either 0.1% methanol or 1 nM LMB for 4 h and either fixed for immunofluorescence microscopy or harvested for the preparation of total cell lysates. A, Western blot of AHR and XAP2 expression in total cell lysates prepared from cells transfected with siCON or XAP2 siRNA (siXAP). B, cells were visualized for AHR. Fixed cells were stained with 1.0 μg/ml A-1 IgG and visualized with GAR-RHO IgG (1:400). The FITC-labeled panels represent the exact fields presented to the left and illustrate the transfection efficiency of the experiment. Scale bar, 10 μm.

that equal amounts of XAP2 can be coprecipitated with the AHR from each of the cell lines regardless of its subcellular localization. Thus, these results confirm that XAP2 can be a component of the unliganded AHR complex when it is localized to the nucleus and suggest that XAP2 does not influence the subcellular localization of the AHR complex when the C-terminal 305 amino acids of the AHR have been removed.

Discussion

The results presented in this report show that endogenous levels of XAP2 can be coprecipitated with the endogenous Ah^{b-1} receptor at time points when the AHR is predominantly localized within the nucleus. Indeed, these time-course studies suggest that there are several different pools of Ah^{b-1} receptor present in the nucleus of Hepa-1 cells after ligand exposure. These include 1) core AHR complexes that remain associated with XAP2, 2) soluble AHRs that are associated with ARNT but not bound to DNA, and 3) AHR·ARNT complexes that are associated with DNA (data not shown; see Pollenz, 1996; Hestermann and Brown, 2003). Thus, it seems that XAP2 does not affect the translocation of the Ah^{b-1} receptor to the nucleus after ligand stimulation, and these studies support the hypothesis that only a small fraction of the ligand-bound AHR actually dimerizes with ARNT during the first 75 min of ligand exposure (Pollenz et al., 1999; Pollenz and Dougherty, 2005). Recent studies suggest that the NLS sequence of the Ah^{b-1} receptor is not masked by the binding of XAP2 but that XAP2 affects AHR localization by perturbing the ability of the NLS domain to actually interact with nuclear import receptors (Petrulis et al., 2003). Thus, the current results suggest that the ligand binding event is able to overcome the conformational change imposed by the association of the AHR with XAP2.

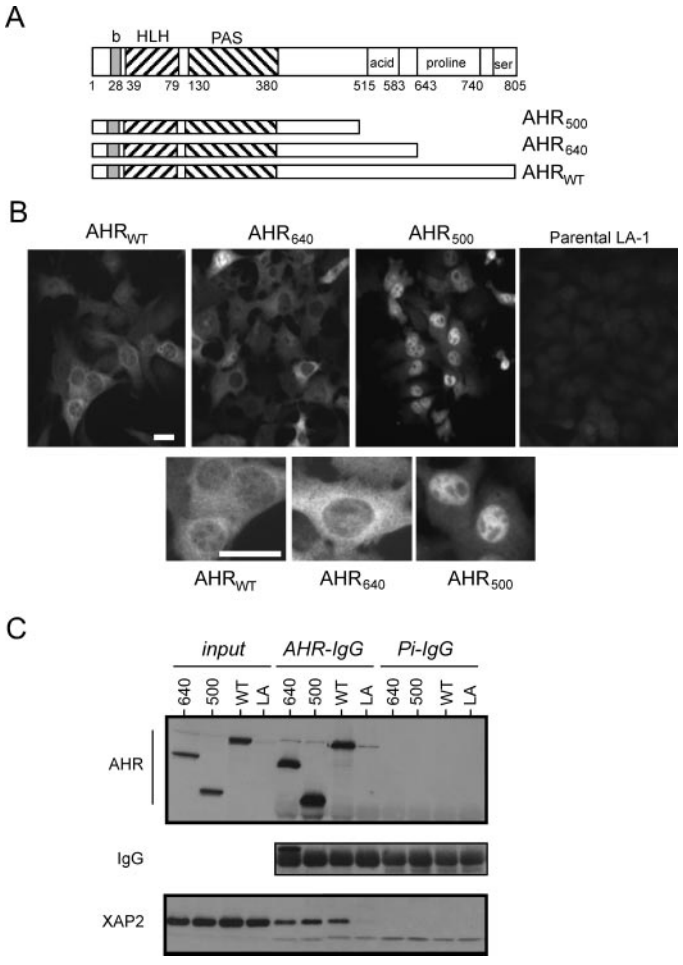

Fig. 7. Localization of AHRs containing C-terminal truncations. A, schematic of the AHR truncations used in the experiments. b, basic region; HLH, helix-loop-helix; PAS, Per-ARNT-Sim domain. Numbers represent amino acids. B, indicated cell lines were fixed and stained with 1.0 μg/ml A-1 IgG and visualized with GAR-RHO IgG (1:400). Scale bar, 5 μm. C, cytosol was prepared from the indicated cell lines, and 600 μg was precipitated with either AHR (Ah-IgG) or preimmune IgG (Pi-IgG) as detailed under *Materials and Methods*. Each of the precipitated samples as well as 15 μg cytosol (input) was resolved by SDS-PAGE and blotted. Blots were stained with either 1.0 μg/ml A-1A IgG or XAP2 mouse IgG$_1$ (1:750), and reactivity was visualized by ECL with GAR-HRP or GAM-HRP IgG (1:10,000). 640, AHR$_{640}$ cell lines; 500, AHR$_{500}$ cell line; WT, AHR$_{WT}$ cell line; LA, LA-I cell line.

The association of XAP2 with the Ah^{b-1} receptor in the nucleus may have functional implications in the signal transduction process, because it may reduce the ability of the receptor population to form functional dimers with ARNT and bind to DNA. Recent studies support this view by showing that the expression of XAP2 actually reduces the level of gene induction mediated by the Ah^{b-1} receptor (Hollingshead et al., 2004; Pollenz and Dougherty, 2005). In addition, the current studies confirm that a soluble pool of Ah^{b-1} receptor complexes can be isolated after extended periods of ligand exposure that remain associated with the same level of XAP2 as unliganded receptors. Because ligand-induced degradation of the AHR seems to require DNA binding (Ma and Baldwin, 2000; Pollenz et al., 2005), the continued association with XAP2 might serve to limit this pool of AHRs from functioning in gene regulation and subsequently being degraded.

Previous studies have suggested that XAP2 is only associated with 40% of the unliganded Ah^{b-1} receptor complex in Hepa-1 cells (Petrulis et al., 2000). However, results presented in the current report show that overexpression of human XAP2 does not lead to increased levels of endogenous Ah^{b-1} receptor or increased levels of total XAP2 protein associated with the endogenous Ah^{b-1} receptor complex. Indeed, the exogenously expressed hXAP2 seems to replace endogenous mXAP2 in the unliganded Ah^{b-1} receptor complex but does not result in an overall increase in the level of XAP2 immunoprecipitated with the AHR. If only 40% endogenous Ah^{b-1} complexes were associated with XAP2, it would be expected that increased XAP2 expression would drive up the level of XAP2 associated with the AHR complex until it was saturated. It is noteworthy that increased association of XAP2 can be observed when similar studies are carried out in cells that express the mouse Ah^{b-2} receptor, because this receptor is associated with 8- to 10-fold less XAP2 than the Ah^{b-1} receptor under endogenous conditions (Pollenz and Dougherty, 2005; R. S. Pollenz, unpublished data). In addition, the results presented in the current report show that the relative XAP2:AHR ratio in the core complex after 4 h of ligand exposure is the same as the ratio in the AHR complex precipitated from untreated cells. If XAP2 were associated with only a small population of receptors and involved in stabilization of that population, it would be expected that XAP2/AHR ratio would increase after prolonged ligand exposure, because 85% of the population has been degraded. Together, these studies support a model in which the majority

of the unliganded Ah^{b-1} receptor complexes are associated with XAP2, and this association temporally limits the "transformation" of the receptors after ligand-induced nuclear localization.

The current studies also support a role of endogenous XAP2 in inhibiting the nucleocytoplasmic shuttling behavior of the endogenous Ah^{b-1} receptor, but they do not support a role for XAP2 in maintaining the unliganded Ah^{b-1} receptor in the cytoplasm of Hepa-1 cells. Indeed, the reduction in endogenous XAP2 by siRNA did not affect the localization of the unliganded Ah^{b-1} receptors, and they remained predominantly localized within the cytoplasm. These results are in contrast to those using transient expression models, where the unliganded Ah^{b-1} receptor exhibits a predominantly nuclear localization in the absence of exogenously expressed XAP2 (Kazlauskas et al., 2000, 2002; Berg and Pongratz, 2002; Petrulis et al., 2003). It is noteworthy that when nuclear export was inhibited in Hepa-1 cells that had reduced levels of XAP2, Ah^{b-1} receptors accumulated within the nucleus. These findings are significant because they directly demonstrate that XAP2 is involved in modulating the nuclear import of the unliganded Ah^{b-1} receptor under endogenous conditions. In addition, these results further support a model in which the majority of the unliganded Ah^{b-1} receptor complexes are associated with XAP2, because unliganded Ah^{b-1} receptor complexes do not accumulate in the nucleus when nuclear export was blocked. Moreover, the results demonstrate that XAP2 is not the sole determinant for whether the unliganded Ah^{b-1} receptor will be localized within the cytoplasmic compartment in the Hepa-1 cell line. The ultimate subcellular location of a target protein with both NLS and NES domains is related to how it interacts with the nuclear import and export machinery in any given cell (for review, see Pemberton and Paschal, 2005). For example, the AHR_{500} can be detected in the nucleus, even when XAP2-associated; thus, in this conformation, nuclear import is clearly favored, and the influence of XAP2 in blocking association with import receptors has been diminished. In addition, when the NLS-GFP-GST-NES protein is expressed in Hepa-1 cells, the protein is predominantly localized to the cytoplasm, even though the protein is clearly being shuttled through the nucleus and has just as much chance of being predominantly localized there. Thus, it is likely that differences in the association of the Ah^{b-1} receptor with the nuclear import and export machinery can explain the nuclear localization of the Ah^{b-1} receptor in COS cells in the absence of XAP2 (Kazlauskas et al., 2000, 2002; Berg and Pongratz, 2002; Petrulis et al., 2003). In summary, these results show that although XAP2 may modulate the ability of the unliganded Ah^{b-1} receptor to undergo dynamic nucleocytoplasmic shuttling, it does not seem to be the sole determinant of AHR localization in Hepa-1 cells. It is important to note that although XAP2 is ubiquitously expressed in all tissues and cell lines tested to date (Carver and Bradfield, 1997; Meyer et al., 1998; Petrulis et al., 2000), it is unclear whether the XAP2/AHR ratio observed in the Hepa-1 cells is the same as that found in tissues. Thus, given the importance of XAP2 as a possible low-penetrance tumor susceptibility gene (Vierimaa et al., 2006), it will be critical to further refine the function of XAP2 in cell culture and tissues and to evaluate its impact on ligand-induced gene regulation mediated by the endogenous Ah^{b-1} receptor as opposed to endogenous AHRs from other species that do not exhibit a high level of association with XAP2.

Acknowledgments

We are grateful to Dr. Stauber for promptly providing pC3-NLS-GFP-GST-RevNES for these studies. Dr. Gary Perdew is gratefully acknowledged for providing the human XAP2 cDNA expression vectors. Jesal Popat is also acknowledged for excellent technical assistance on some of the experiments.

References

Bell DR and Poland A (2000) Binding of aryl hydrocarbon receptor (AhR) to AhR-interacting protein. The role of hsp90. *J Biol Chem* **275:**36407–36414.

Berg P and Pongratz I (2002) Two parallel pathways mediate cytoplasmic localization of the dioxin (aryl hydrocarbon) receptor. *J Biol Chem* **277:**32310–32319.

Carver LA and Bradfield CA (1997) Ligand-dependent interaction of the aryl hydrocarbon receptor with a novel immunophilin homolog in vivo. *J Biol Chem* **272:** 11452–11456.

Carver LA, LaPres JJ, Jain S, Dunham EE, and Bradfield CA (1998) Characterization of the Ah receptor-associated protein, ARA9. *J Biol Chem* **273:**33580–33587.

Davarinos NA and Pollenz RS (1999) Aryl hydrocarbon receptor imported into the nucleus following ligand binding is rapidly degraded via the cytoplasmic proteasome following nuclear export. *J Biol Chem* **274:**28708–28715.

Davies TH and Sanchez ER (2005) FKBP52. *Int J Biochem Cell Biol* **37:**42–47.

Elbi C, Misteli T, and Hager GL (2002) Recruitment of dioxin receptor to active transcription sites. *Mol Biol Cell* **13:**2001–2015.

Giannone JV, Okey AB, and Harper PA (1995) Charcaterization of polyclonal antibodies to the aromatic hydrocarbon receptor. *Can J Physiol Pharmacol* **73:**7–17.

Hestermann E and Brown M (2003) Agonist and chemopreventive ligands induce differential transcriptional cofactor recruitment by the aryl hydrocarbon receptor. *Mol Cell Biol* **23:**7920–7925.

Hollingshead BD, Petrulis JR, and Perdew GH (2004) The aryl hydrocarbon (Ah) receptor transcriptional regulator hepatitis B virus X-associated protein 2 antagonizes p23 binding to Ah receptor-Hsp90 complexes and is dispensable for receptor function. *J Biol Chem* **279:**45652–45661.

Holmes JL and Pollenz RS (1997) Determination of aryl hydrocarbon receptor nuclear translocator protein concentration and subcellular localization in hepatic and nonhepatic cell culture lines: development of quantitative Western blotting protocols for calculation of aryl hydrocarbon receptor and aryl hydrocarbon receptor nuclear translocator protein in total cell lysates. *Mol Pharmacol* **52:**202–211.

Kazlauskas A, Poellinger L, and Pongratz I (2000) The immunophilin-like protein XAP2 regulates ubiquitination and subcellular localization of the dioxin receptor. *J Biol Chem* **275:**41317–41324.

Kazlauskas A, Poellinger L, and Pongratz I (2002) Two distinct regions of the immunophilin-like protein XAP2 regulate dioxin receptor function and interaction with hsp90. *J Biol Chem* **277:**11795–11801.

Knauer SK, Moodt S, Berg T, Liebel U, Pepperkok R, and Stauber RH (2005) Translocation biosensors to study signal-specific-nucleo-cytoplasmic transport, protease activity, and protein-protein interactions. *Traffic* **6:**594–606.

Kudo N, Wolff B, Sekimoto T, Schreiner EP, Yoneda Y, Yanagida M, Horinouchi S, and Yoshida M (1998) Leptomycin B inhibition of signal-mediated nuclear export by direct binding to CRM1. *Exp Cell Res* **242:**540–547.

Kudo N, Khochbin S, Nishi K, Kitano K, Yanagida M, Yoshida M, and Horinouchi S (1997) Molecular cloning and cell cycle-dependent expression of mammalian CRM1, a protein involved in nuclear export of proteins. *J Biol Chem* **27:**29742–29751.

LaPres JJ, Glover E, Dunham EE, Bunger MK, and Bradfield CA (2000) ARA9 modifies agonist signaling through an increase in cytosolic aryl hydrocarbon receptor. *J Biol Chem* **275:**6153–6159.

Ma Q and Baldwin KT (2000) 2,3,7,8-tetrachlorodibenzo-p-dioxin-induced degradation of aryl hydrocarbon receptor (AhR) by the ubiquitin-proteasome pathway. Role of the transcription activation and DNA binding of AhR. *J Biol Chem* **275:** 8432–8438.

Ma Q and Whitlock JP Jr (1997) A novel cytoplasmic protein that interacts with the Ah receptor, contains tetratricopeptide repeat motifs, and augments the transcriptional response to 2,3,7,8-tetrachlorodibenzo-p-dioxin. *J Biol Chem* **272:**8878–8884.

Meyer BK and Perdew GH (1999) Characterization of the AhR-hsp90-XAP2 core complex and the role of the immunophilin-related protein XAP2 in AhR stabilization. *Biochemistry* **38:**8907–8917.

Meyer BK, Petrulis JR, and Perdew GH (2000) Aryl hydrocarbon (Ah) receptor levels are selectively modulated by hsp90-associated immunophilin homolog XAP2. *Cell Stress Chaperones* **5:**243–254.

Meyer BK, Pray-Grant MG, Vanden Heuvel JP, Perdew GH (1998) Hepatitis B virus X-associated protein 2 is a subunit of the unliganded aryl hydrocarbon receptor core complex and exhibits transcriptional enhancer activity. *Mol Cell Biol* **18:**978–988.

Paine PL, Austerberry CF, Desjarlais LJ, and Horowitz SB (1983) Protein loss during nuclear isolation. *J Cell Biol* **97:**1240–1242.

Pemberton LF and Paschal BM (2005) Mechanisms of receptor-mediated nuclear import and nuclear export. *Traffic* 2005 **6:**187–198.

Petrulis JR, Hord NG, and Perdew GH (2000) Subcellular localization of the aryl hydrocarbon receptor is modulated by the immunophilin homolog hepatitis B virus X-associated protein 2. *J Biol Chem* **275:**37448–37453.

Petrulis JR, Kusnadi A, Ramadoss P, Hollingshead B, and Perdew GH (2003) The hsp90 Co-chaperone XAP2 alters importin β recognition of the bipartite nuclear

localization signal of the Ah receptor and represses transcriptional activity. *J Biol Chem* **278:**2677–2685.
Petrulis JR and Perdew GH (2002) The role of chaperone proteins in the aryl hydrocarbon receptor core complex. *Chem Biol Interact* **141:**25–40.
Pollenz RS (1996) The aryl hydrocarbon receptor but not Arnt protein is rapidly depleted in hepatic and non hepatic culture cells exposed to 2,3,7,8-tetrachlorodibenzo-p-dioxin. *Mol Pharmacol* **49:**391–398.
Pollenz RS, Davarinos NA, and Shearer TP (1999) Analysis of AHR-mediated signaling under physiological hypoxia reveals lack of competition for the ARNT transcription factor. *Mol Pharmacol* **56:**1127–1137.
Pollenz RS and Dougherty EJ (2005) Redefining the role of XAP2 and CHIP in the degradation of endogenous AHR in cell culture models. *J Biol Chem* **280:**33346–33356.
Pollenz RS, Popet J, and Dougherty EJ (2005) Role of the carboxy-terminal transactivation domain and active transcription in the ligand-induced degradation of the mouse Ah^{b-1} receptor. *Biochem Pharmacol* **70:**1623–1633.
Pollenz RS, Santostefano MJ, Klett E, Richardson V, Necela B, and Birnbaum LS (1998) A single oral dose of TCDD results in sustained depletion of AHR protein in female Sprague-Dawley rats. *Toxicol Sci* **42:**117–128.
Pollenz RS, Santostefano MJ, Klett E, Richardson VM, Necela B, Birnbaum LS (1998) Female Sprague Dawley rats exposed to a single oral dose of 2,3,7,8-tetrachlorodibenzo-p-dioxin exhibit sustained depletion of aryl hydrocarbon receptor protein in liver, spleen, thymus and lung. *Toxicol Sci* **42:**117–128.
Pollenz RS, Sattler CA, and Poland A (1994) The aryl hydrocrabon receptor and aryl hydrocarbon receptor nuclear translocator protein show distinct subcellular localization in Hepa 1c1c7 cell by immunofluorescence microscopy. *Mol Pharmacol* **45:**428–438.
Ramadoss P, Petrulis JR, Hollingshead BD, Kusnadi A, and Perdew GH (2004) Divergent roles of hepatitis B virus X-associated protein 2 (XAP2) in human versus mouse Ah receptor complexes. *Biochemistry* **43:**700–709.
Song Z and Pollenz RS (2002) Ligand dependent and independent modulation of AH receptor localization, degradation, and gene regulation. *Mol Pharmacol* **62:**806–816.
Vierimaa O, Georgitsi M, Lehtonen R, Vahteristo P, Kokko A, Raitila A, Tuppurainen K, Ebeling TM, Salmela PI, Paschke R, et al. (2006) Pituitary adenoma predisposition caused by germline mutations in the AIP gene *Science (Wash DC)* **312:**1228–1230.

Address correspondence to: Dr. Richard S. Pollenz, Department of Biology, BSF 110, 4202 E. Fowler Ave., University of South Florida, Tampa, FL 33620. E-mail: pollenz@cas.usf.edu